land

MDPI

Article

Integrating Blue–Green Infrastructure with Gray Infrastructure for Climate-Resilient Surface Water Flood Management in the Plain River Networks

Liqing Zhu [1], Chi Gao [2,*], Mianzhi Wu [1] and Ruiming Zhu [3]

[1] Department of Landscape Architecture, Shanghai Jiao Tong University, Shanghai 200240, China; lqzhu88@sjtu.edu.cn (L.Z.); wumianzhi@sjtu.edu.cn (M.W.)
[2] Department of Landscape Architecture, Huazhong Agricultural University, Wuhan 430070, China
[3] Department of Computer Science, Illinois Institute of Technology, Chicago, IL 60647, USA; rzhu8@hawk.iit.edu
* Correspondence: gaochi@mail.hzau.edu.cn

Abstract: Along with the progression of globalized climate change, flooding has become a significant challenge in low-lying plain river network regions, where urban areas face increasing vulnerability to extreme climate events. This study explores climate-adaptive land use strategies by coupling blue–green infrastructure (BGI) with conventional gray infrastructure, forming blue–green–gray infrastructure (BGGI), to enhance flood resilience at localized and regional scales. By integrating nature-based solutions with engineered systems, this approach focuses on flood mitigation, environmental co-benefits, and adaptive land-use planning. Using the Minhang District in Shanghai as a case study, the research employs geospatial information system (GIS) analysis, hydrological modeling, and scenario-based assessments to evaluate the performance of BGGI systems under projected climate scenarios for the years 2030, 2050, and 2100. The results highlight that coupled BGGI systems significantly improve flood storage and retention capacity, mitigate risks, and provide ecological and social benefits. Water surface-to-catchment area ratios were optimized for primary and secondary catchment areas, with specific increases required in high-risk zones to meet future flood scenarios. Ecological zones exhibited greater adaptability, while urban and industrial areas required targeted interventions. Scenario-based modeling for 2030, 2050, and 2100 demonstrated the scalability, feasibility, and cost-effectiveness of BGI in adapting to climate-induced flooding. The findings contribute to the existing literature on urban flood management, offering a framework for climate-adaptive planning and resilience building with broader implications for sustainable urban development. This research supports the formulation of comprehensive flood management strategies that align with global sustainability objectives and urban resilience frameworks.

Keywords: climate-adaptive strategies; land use; blue–green–gray infrastructure; GIS analysis; hydrological modeling; scenario-based assessments; flood resilience

Academic Editors: Xiwei Shen, Bo Zhang and Yang Song

Received: 19 February 2025
Revised: 12 March 2025
Accepted: 13 March 2025
Published: 17 March 2025

Citation: Zhu, L.; Gao, C.; Wu, M.; Zhu, R. Integrating Blue–Green Infrastructure with Gray Infrastructure for Climate-Resilient Surface Water Flood Management in the Plain River Networks. *Land* **2025**, *14*, 634. https://doi.org/10.3390/land14030634

1. Introduction

The frequency and intensity of extreme climate events, driven by global climate change, present serious challenges for urban water management systems worldwide [1]. This is particularly evident in low-lying plain river network regions, where urban flooding has become a recurrent and significant problem. As these areas face increasing pressure from rapid urbanization and climate variability, there is an urgent need for adaptive strategies

that enhance resilience and mitigate flood risks [2]. Adopting climate-responsive land use strategies that incorporate resilient infrastructure is crucial for effectively addressing these vulnerabilities.

One promising solution is the integration of blue–green infrastructure (BGI) with conventional gray infrastructure—a hybrid approach that optimizes urban flood management. BGI serves as a network of green and blue spaces, providing multiple ecosystem services to create more sustainable urban environments [3] and exemplifying nature-based solutions. Grounded in scientific principles, nature-based solutions incorporate various natural elements and processes to enhance the resilience of urban spaces and improve human well-being [4,5]. BGI encompasses features such as green roofs, permeable pavements, rain gardens, and wetlands, which enhance water infiltration, storage, and purification processes [5–7]. Gray infrastructure, which includes engineered systems such as drainage pipes, levees, and stormwater reservoirs, provides the structural foundation necessary for managing extreme flood events. The integration of these systems into blue–green–gray infrastructure (BGGI) enables an adaptive, scalable, and cost-effective approach to urban flood resilience [5–7]. By harmonizing natural and engineered systems, BGGI offers a comprehensive framework for addressing urban flood challenges, facilitating optimized flood mitigation, enhanced ecological functions, and improved resilience in response to climate uncertainties [8]. Through effective integration, blue–green systems can regulate and absorb excess surface water, while gray infrastructure provides the necessary structural support to direct and control water flow during extreme events [9].

Additionally, the integration of small- to medium-scale BGGI systems has proven effective for targeted flood mitigation, offering cities a scalable, adaptable, and context-specific method to address the unique hydrological needs of their local environments [10,11]. Small- to medium-scale BGGI systems refer to localized interventions implemented at the level of individual buildings, neighborhoods, or specific urban districts [12,13]. Examples include installing green roofs or rain gardens on buildings or streets, implementing permeable pavements in parking lots or sidewalks, and designing localized wetlands to manage runoff in specific neighborhoods. These systems contrast with large-scale flood management interventions, such as city-wide stormwater management networks or extensive flood barriers along entire riverbanks.

The primary advantage of small- to medium-scale BGGI interventions lies in their flexibility. They can be customized to address site-specific challenges, implemented incrementally, and seamlessly integrated into existing urban layouts without requiring extensive infrastructure overhaul. This adaptability makes them particularly suitable for high-density urban environments, where large-scale solutions may be impractical due to space constraints or economic limitations.

Despite the demonstrated benefits of BGGI, several gaps remain in the literature regarding its application in densely populated and socioeconomically diverse urban areas. Current research primarily focuses on specific case studies or isolated BGI solutions, with limited emphasis on the effectiveness of small- to medium-scale systems in high-density urban settings. Additionally, while multi-objective frameworks provide useful guidance for decision-making, further research is needed to validate these models across different climates, urban morphologies, and topographical conditions.

This study aims to address these gaps by exploring the coupling of small- to medium-scale BGGI systems for flood resilience in plain river network regions, with a particular focus on Shanghai and the surrounding areas. By applying a multi-objective analytical framework and evaluating a range of urban contexts, this research contributes to a more comprehensive understanding of BGGI implementation and provides insights into scalable climate-adaptive land use planning strategies.

2. Literature Review

In recent years, urban resilience has emerged as a central theme in climate adaptation, driven by the increasing frequency of extreme weather events and their impact on urban infrastructure. The concept of resilience, originally rooted in ecology and engineering, refers to a system's ability to absorb, adapt, and recover from disturbances while maintaining essential functions [14]. In urban contexts, resilience specifically addresses how cities can withstand, adapt to, and recover from various disruptions, particularly climate-related hazards like flooding. This section reviews the literature on resilient urban theory, blue–green–gray infrastructure strategies, and the theoretical analysis framework with integrated approaches to flood management.

2.1. Resilient Urban Theory and Evolution

The majority of the world's population resides in urban areas, making cities particularly susceptible to extreme weather events such as storm surges and heat waves. Urban environments, economies, and social systems remain highly sensitive to these events, whose impacts are further intensified by climate change. Among these challenges, flooding presents significant risks and uncertainties, especially under evolving climate conditions. Traditional flood control strategies often prove inadequate during catastrophic flooding, exposing coastal cities to severe threats to both life and assets. The compounding effects of sea-level rise, persistent land subsidence, and intensified storm surges further exacerbate the disastrous consequences of climate change. While conventional flood control measures are often costly, climate adaptation strategies designed to mitigate flood impacts tend to be more economically sustainable [15].

A shift from a flood resistance-focused approach to one that incorporates flood accommodation aims to promote urban development that is both ecologically intelligent and aligned with sustainable, adaptive practices. The concept of resilience, derived from the Latin term *resilire* (to leap back), originally referred to a material's capacity to return to its original shape after deformation. Over time, the term evolved within disciplines such as social sciences, ecology, and urban planning to describe the ability of systems to absorb, adapt to, and recover from disturbances. Holling's foundational work distinguished between two types of resilience: ecological resilience, which emphasizes recovery and persistence, and engineering resilience, which focuses on stability and rapid return to equilibrium after disturbances [16].

Urban resilience builds upon these principles, addressing the interconnected social, economic, and environmental complexities of urban systems. Specifically, flood resilience refers to an urban system's ability to absorb or adapt to flood events while maintaining functionality, whereas climate resilience encompasses a city's broader capacity to withstand and recover from climate-related impacts [17]. Scholars such as Jabareen have examined resilience through multidisciplinary frameworks, integrating ecological, social, and economic perspectives to assess urban adaptive capacities [18]. These perspectives highlight the dynamic relationship between physical infrastructure and social dynamics in fostering urban resilience.

Cities that adopt resilience-based strategies are better positioned to adapt to floods and recover from large-scale flood events [19]. However, urban resistance strategies and resilience strategies represent fundamentally distinct approaches. With the accelerating pace of urbanization, urban flood management has been dominated by reliance on gray infrastructure and traditional flood resistance measures. This has resulted in challenges such as the continual elevation of levees, increasing population density in vulnerable areas, and cost inefficiencies. Given the uneven distribution of flood risk across urban landscapes, this study argues that resistance and resilience strategies should be viewed as

complementary rather than mutually exclusive, blending structural rigidity with adaptive flexibility. Coastal cities, in particular, can adopt a hybrid approach to address climate-related challenges, allowing them to achieve both flood resistance and enhanced functional redundancy to withstand large-scale socio-economic disruptions.

2.2. Urban Infrastructure for Urban Flood Resilience

Urban blue infrastructure, particularly in waterfront areas, typically consists of interconnected water bodies such as river networks, lakes, and ponds. These systems can be categorized into three primary spatial forms: (1) scattered distribution, where water bodies are dispersed without direct connectivity; (2) lake–river systems, characterized by the connection of rivers and lakes, with large lakes playing a significant role in supporting urban development; and (3) river networks, where an interconnected system of rivers dominates the landscape. Composite forms also exist, combining these patterns, such as scattered and networked water bodies or lake–river systems with river networks.

The functionality of blue infrastructure varies with its spatial form (Figure 1). Scattered water bodies, for instance, often face challenges in flood management due to their limited capacity to handle overflow, necessitating on-site flood absorption. In contrast, interconnected systems like lake–river and river networks facilitate flood detention and drainage.

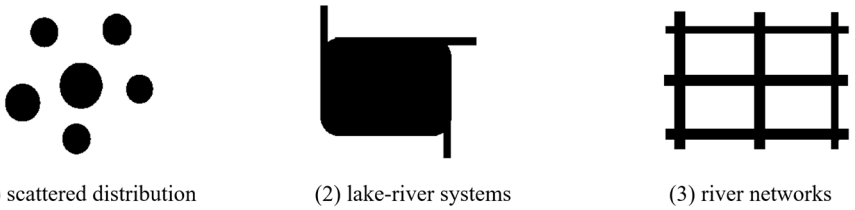

Figure 1. Three basic forms of blue space in the Huangpu River waterfront [20].

Blue infrastructure functions across various spatial scales—macro, meso, and micro—each serving distinct roles in urban flood resilience. At the macroscale, large water bodies, such as artificial lakes spanning several square kilometers, play a critical role in city-wide flood management. Notable examples include West Lake in Hangzhou (6.38 km^2) and Dishui Lake in Shanghai (5.56 km^2), which exceed the typical scale of waterfront spaces, providing strategic flood storage and drainage for their respective cities. At the mesoscale, blue spaces within regional catchment areas contribute to flood resilience by serving as key components of urban and suburban drainage systems. These water bodies, often a few hectares in size, function as central hydrological features that regulate stormwater flow. For instance, Lanshang Lake in Wujing Town, Shanghai, which covers 40 hectares, plays a significant role in flood storage within its catchment area. At the microscale, blue infrastructure consists of small ponds or localized water bodies within sub-catchment areas, often enclosed by local roads, walls, or channels. These smaller-scale interventions provide localized flood mitigation by enhancing water retention and infiltration within urban neighborhoods.

Despite growing research on urban resilience, significant knowledge gaps persist regarding the integration of blue–green infrastructure with traditional gray infrastructure. Current studies often focus on isolated solutions without examining how interactions between blue–green and gray infrastructure can enhance flood resilience. Furthermore, few studies systematically evaluate how hybrid infrastructure systems respond to climate variability, particularly in highly urbanized settings. Additionally, empirical research on the long-term effectiveness of integrated blue–green–gray infrastructure remains limited, particularly regarding its real-world performance under varying climatic conditions. This study seeks to address these gaps by investigating the direct and indirect impact

mechanisms of blue–green–gray infrastructure integration, offering insights into its role in adaptive flood management strategies.

2.3. Blue–Green–Gray Infrastructure for Urban Flood Resilience

The coupling of BGGI has gained traction as an effective means to increase urban resilience, particularly in areas prone to flooding. Blue infrastructure, which includes natural water systems such as rivers, lakes, and wetlands, works in tandem with green infrastructure—vegetated areas that promote natural processes like water infiltration, purification, and cooling. The combination of blue and green elements with gray infrastructure, such as pipes, levees, and stormwater drains, creates a multifaceted flood management approach. This approach allows for the regulation of excess water during heavy rainfall, while gray infrastructure provides essential structural support and control [21].

Multi-Objective Decision-Making Frameworks in BGGI Design

Effective design and implementation of BGGI require multi-objective decision-making frameworks to balance environmental benefits with performance and cost-efficiency. These frameworks allow urban planners to consider factors such as rainfall intensity, system performance, maintenance costs, and the spatial distribution of infrastructure. Husnain et al. demonstrated how multi-objective frameworks could optimize green–gray infrastructure for urban drainage, providing a decision-making basis that maximizes resilience while controlling expenses [22]. The framework addresses the need for sustainable solutions, helping planners to make informed choices about infrastructure investments that align with long-term resilience goals. Using such frameworks can also enhance the functionality of urban drainage systems (UDS), which are often limited by capacity constraints and aging infrastructure in high-density urban areas [23]. By incorporating green–gray infrastructure into decision models, urban planners can evaluate different configurations that reduce the urban heat island effect, enhance ecosystem services, and ultimately contribute to a city's adaptability and resilience.

3. Research Design

This study adopts a theoretical framework that examines the underlying rationale for integrating blue–green infrastructure with gray infrastructure in flood management. This integration enhances urban flood resilience through two primary pathways: the direct impact mechanism and the indirect impact mechanism.

The direct impact mechanism refers to the immediate and measurable effects of BGGI integration on urban flood resilience. The synergistic combination of permeable surfaces, water retention basins, and green spaces with traditional gray infrastructure enhances stormwater absorption, reduces runoff volume, and improves drainage efficiency. These integrated systems extend the operational lifespan of urban drainage networks by alleviating pressure on existing flood control structures. The interaction between blue–green and gray elements also leads to better peak flow regulation and enhanced water quality management through natural filtration processes.

Beyond immediate flood mitigation, the integration of blue–green and gray infrastructure generates indirect benefits that contribute to urban resilience. Green spaces and permeable surfaces enhance biodiversity, promote climate adaptation, and create co-benefits such as urban cooling and carbon sequestration. These features also contribute to public health and social well-being by providing recreational spaces and enhancing aesthetic value. The economic benefits of integrating blue–green infrastructure include increased property values and reduced long-term maintenance costs for flood control infrastructure.

The methodological framework of this study includes (1) using GIS 10.5 software for current situation analysis and catchment area delineation; (2) conducting surface water rate and flood adaptability assessments of each site based on historical flood data and climate change scenario predictions for 2030, 2050 and 2100; (3) comparing the flood adaptability of the sites before and after redevelopment to identify improvement opportunities and potential challenges. Through this comprehensive methodology, the study aims to provide scientific evidence and practical guidance for climate adaptation planning and the management of urban waterfront areas in the context of climate change.

This research utilized a case study approach, providing a framework for contextualizing and evaluating the application of blue–green–gray infrastructure in a real-world setting. The selected study area is in Shanghai's Minhang District, a region within the plain river network area of southern China. As a rapidly urbanizing area with significant exposure to flooding risks, Minhang District provides a representative environment for evaluating the effectiveness of small- to medium-scale BGGI systems.

This case study facilitates an in-depth analysis of the area's environmental, hydrological, and socio-economic conditions—factors that are often difficult to fully capture through theoretical or generalized approaches. Examining plain river regions in southern China sheds light on the unique challenges of flood-prone urban areas, including the complex interactions between rainfall intensity, urban density, and existing infrastructure. By applying a rigorous case-study approach, the performance and adaptability of coupled BGGI systems can be thoroughly assessed, providing empirical insights into their effectiveness for optimizing flood mitigation while delivering environmental co-benefits. Moreover, this approach ensures that the proposed multi-objective decision-making framework is both theoretically robust and practically feasible. The findings generated from this case study establish a solid foundation for extending the applicability of BGGI strategies to similar urban and hydrological contexts, thereby contributing to the broader discourse on sustainable urban development and resilience building.

This research also examines catchment delineation, water surface design, and storage capacities across ten selected sub-catchments. A comparative analysis of water surface ratios provides insights into the adaptive capacities of each site under projected climate change scenarios. By synthesizing these findings, the study explores how Minhang's diverse land-use patterns can be leveraged to enhance urban flood resilience through tailored BGGI strategies.

3.1. Case Study Context: Minhang District, Shanghai

Located in the north subtropical humid monsoon climate zone and the lower Yangtze River Delta, Shanghai's Minhang District frequently experiences flood challenges due to its flat terrain, high water table, and extensive river network. Covering an area of approximately 371 square kilometers, the district includes key waterways such as the Huangpu River, which plays a critical role in shaping its hydrological patterns. Minhang encompasses diverse land uses, ranging from densely populated urban zones and industrial areas to agricultural lands and emerging commercial districts, making it an ideal area for studying urban flood resilience.

For this study, ten representative catchment areas (CA: A–I) along the Huangpu River were selected based on their flood vulnerability, land use diversity, and infrastructural characteristics (Figure 2). These sites are categorized into three types, as follows:

- Built-up areas (CA: A,B,E,F): urban zones with high-density residential, commercial, and industrial land use, where gray infrastructure dominates. Three sub-catchments within this category are located in fully developed urban areas slated for partial waterfront redevelopment.

- Transitional areas (CA: D,G,H,I): newly developed or under-development sites designated for mixed land use as part of Shanghai's 14th Five-Year Plan. Three sub-catchments represent these areas, where ongoing or planned development reflects the city's urban expansion.
- Preserved green zones (CA: C,J): agricultural or natural areas with minimal construction, focusing on ecological conservation. Three sub-catchments within this category are located in Pujing Country Park, emphasizing the integration of ecological and hydrological functions.

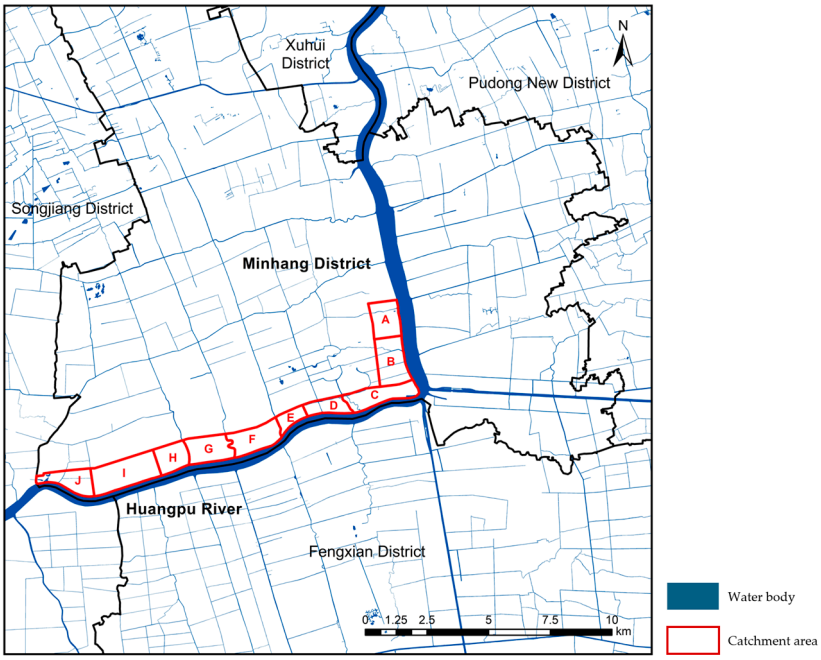

Figure 2. An enlarged view of the distribution of the 10 catchments [19].

Each catchment area spans 0.7 to 3.0 square kilometers and exhibits distinct hydrological and infrastructural characteristics, providing a comprehensive framework for analyzing the impact of BGGI interventions under climate change scenarios.

The design framework for BGGI was tailored to Minhang District's unique hydrological, ecological, and urban contexts. It integrated blue infrastructure, such as retention basins and wetlands, to store and regulate water flow; green infrastructure, including vegetated swales and permeable pavements, to enhance infiltration and ecological connectivity; and gray infrastructure, such as stormwater drains and levees, to channel excess water effectively.

3.2. Data Collection Methods

This study employs diverse datasets and analytical tools to assess urban flood resilience in Shanghai's Minhang District. The integration of high-precision data, field validation, and advanced modeling ensures a robust evaluation of current and future hydrological conditions.

The data sources include engineering blueprints and drainage network diagrams from the Shanghai Drainage Bureau, which provide foundational information on the district's existing gray infrastructure for understanding drainage system capacities and their limitations under various conditions.

Baseline topographical and hydrological data were sourced from the 2016 surveys conducted by the Shanghai Planning and Natural Resources Bureau. These surveys provided detailed measurements essential for delineating catchment areas, calculating water

surface ratios, and analyzing drainage patterns. A consistent dataset from 2016 was selected to ensure comparability across all ten study sites. Engineering blueprints and drainage network diagrams from the Shanghai Drainage Bureau supplemented these datasets, providing insights into the existing gray infrastructure and its integration with natural hydrological features. This information was critical for validating GIS-based analyses and hydrological simulations.

Among the built-up areas (CA: A,B,E,F), site "C" is situated at a pivotal confluence where the Huangpu River makes a sharp turn from an eastward to a northward flow, eventually merging with the Yangtze River at the Wusongkou estuary and discharging into the East China Sea. In the mid-20th century, two artificial waterways were constructed at this site to alleviate flooding pressure on Shanghai's densely populated central districts: the Da Zhi River (flowing eastward) and the Jin Hui Harbor (flowing southward). These channels significantly enhanced flood discharge capacity, reducing flood risks in the city's core.

Within site "A", a central feature is Lanxiang Lake, which was planned and excavated as part of the area's redevelopment. Construction of the lake began in 2018, and the water body was largely completed by late 2020. The data from after this redevelopment will be used for comparison across all sites.

Flood data were drawn from Wang Jun's climate change risk assessments (2012, 2020) [24,25], which modeled flood scenarios under the compounded effects of sea-level rise, land subsidence, and storm surges. Simulations for 2030, 2050, and 2100 provide projections of flood depth, extent, and duration. These datasets were critical for scenario planning and evaluating the effectiveness of blue–green–gray infrastructure (BGGI) interventions.

Lastly, policy directives from the Shanghai Urban Master Plan (2017–2035) [26] were used to align the study's findings with broader urban resilience goals. This framework ensured site-specific interventions were contextualized within the city's strategic vision for sustainable development.

3.3. Research Methods

The methodological framework combines spatial analysis, hydrological modeling, and scenario-based assessments to evaluate flood resilience and the effectiveness of BGGI interventions. The integration of these methods ensures a comprehensive evaluation of current conditions and future adaptability.

3.3.1. GIS Analysis for Current Conditions and Catchment Delineation

GIS technology was employed to delineate catchment areas and analyze spatial characteristics. Due to the flat terrain and complex hydrological networks of Minhang District, standard digital elevation model (DEM) data alone were insufficient to capture the runoff pathways with precision. To overcome this, the study employed the refined digital elevation model (RIDEM), as proposed by Duke et al. and Zuo et al., an enhanced variation of a standard DEM model that integrates surface features such as roads, embankments, and waterways into elevation data for more precise hydrological and terrain analysis [27,28].

The DEM refinement process adjusted elevation values to reflect the influence of anthropogenic and natural features on runoff [29,30]. High-elevation features such as roads and embankments were raised, while low-lying features like ponds and drainage channels were lowered. This approach improved the accuracy of hydrological analyses, enabling the delineation of catchment boundaries that aligned more closely with real-world conditions.

The refined DEM was imported into ArcGIS for hydrological analysis. Using the D8 algorithm [31,32], flow direction and accumulation were calculated to identify runoff pathways and critical flood-prone zones. Digital water networks were extracted and

validated against observed hydrological patterns to ensure accuracy. These analyses formed the foundation for understanding drainage dynamics across the study sites.

Using catchment area A as an example, the GIS analysis began by extracting digital water networks, revealing a dispersed and relatively uniform drainage pattern (Figure 3). These water networks formed the basis for subsequent catchment delineation. Using hydrological tools in ArcGIS, the study employed the D8 algorithm to analyze flow direction and accumulation, identifying runoff pathways and delineating primary (Level 1) and secondary (Level 2) catchments. These results were compared for the pre- and post-construction states of catchment area A to evaluate how the intervention affected runoff dynamics.

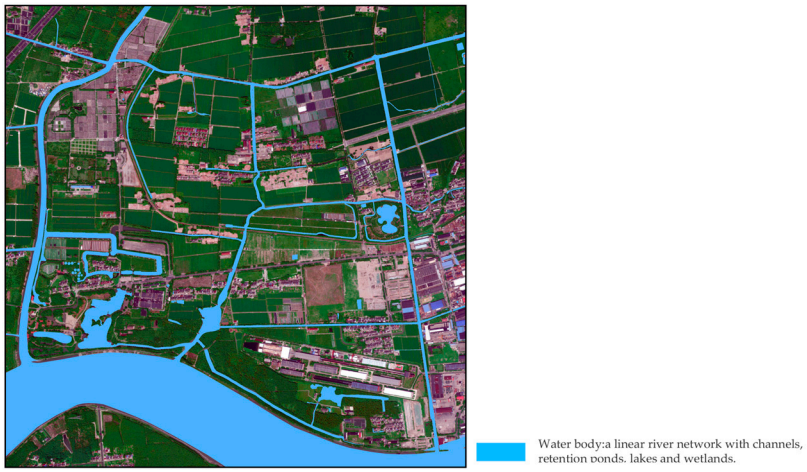

Figure 3. The distribution of linear river network and scattered points in Pujiang Town, Minghang District, Shanghai (Source: modified from Baidu Maps, light blue part represents water body).

Statistical calculations and drainage network measurements were conducted to quantify the composition of blue, green, and gray infrastructure at each site. For catchment area A, the metrics included the proportion of water surface area, green spaces such as agricultural lands and parks, and existing drainage pipelines. The analysis also examined impervious surfaces, such as buildings and hardscapes, to assess their impact on runoff and infiltration. These metrics reflected the balance between permeable and non-permeable surfaces, providing critical insights into flood resilience capacity.

3.3.2. Surface Water Rate and Flood Adaptability Assessments

To evaluate the effectiveness of BGGI interventions, surface water rates and flood adaptability were assessed using hydrological simulations and scenario analysis. The MIKE21 hydrodynamic model, known for its accuracy in urban flood modeling, was employed to simulate flood conditions under current and projected scenarios [33,34]. The model was calibrated using historical rainfall and runoff data from Minhang District, ensuring that parameters such as surface roughness, soil infiltration rates, and water table levels accurately reflected local conditions. This calibration is necessary for replicating observed flood behavior and establishing a reliable baseline for future projections.

Simulations were conducted for 2030, 2050, and 2100, incorporating anticipated increases in rainfall intensity and changes in river flow due to climate change [35]. Baseline scenarios were compared with BGGI-enhanced configurations to assess the interventions' impact on flood risk reduction. Key outputs, including flood depth, spatial extent, and inundation duration, were analyzed to evaluate the potential of BGGI components to mitigate peak flood levels and improve drainage system performance.

Statistical analyses quantified the composition and distribution of blue, green, and gray infrastructure within each catchment. Water surface ratios were calculated to assess retention capacity, while impervious surfaces were analyzed to identify areas less conducive to infiltration and flood absorption. These metrics provided a comprehensive understanding of each site's hydrological dynamics and its capacity to adapt to projected climate scenarios.

3.3.3. Resilience Assessment and Validation

The established multi-objective decision-making framework was implemented to optimize the design and placement of BGGI systems, balancing flood resilience with economic and social considerations. This framework evaluated multiple performance indicators, beginning with the selection of indicators across three categories: environmental (flood risk reduction, water quality improvement, and biodiversity support), economic (cost-effectiveness, maintenance costs, and flood damage mitigation), and social (public accessibility, aesthetic appeal, and community health and well-being). Using the analytical hierarchy process (AHP), weights were assigned to each indicator based on input from urban planning and hydrology experts, and scores for each BGGI configuration were calculated to allow for comparative analysis across different designs [36]. This decision-making framework was then used to identify the most resilient and cost-effective BGGI configurations, optimizing flood risk reduction while maximizing environmental and social co-benefits, thus effectively balancing resilience goals with practical and financial considerations.

3.3.4. Model Development and Calculation Methods

At the catchment level, the study utilizes the rational method to calculate design rainwater flow, accounting for spatial and temporal rainfall distribution variations as well as the effects of drainage network convergence [37,38]. For smaller, secondary catchment areas, the volume method is used based on flow runoff coefficients, with the support of SWMM5.1.014 and ArcGIS10.5 software [38–41]. The calculations are based on the following formulas:

1. Rational Method:

$$Qs = q \cdot \Psi \cdot F \tag{1}$$

In this equation, Qs refers to design rainwater flow (L/s); q stands for design rainfall intensity [L/(s·hm^2)]; Ψ denotes runoff coefficient; and F refers to catchment area (hm^2).

2. Volume Method

$$V = 10n = 1\sum m(Fn \cdot \Psi n) \cdot H \tag{2}$$

Here, V describes design storage volume (m^3); H stands for design rainfall (mm); Ψn means runoff coefficient for each surface type; and Fn refers to area of each surface type n (hm^2).

Through this methodological framework, this study aims to offer scientifically grounded insights and practical support for urban flood risk management and the strategic planning of blue–green–gray infrastructure.

4. Results

The results of the model simulations and empirical data collection were analyzed to evaluate the performance of BGGI in enhancing flood resilience (Figure 4) (Table 1).

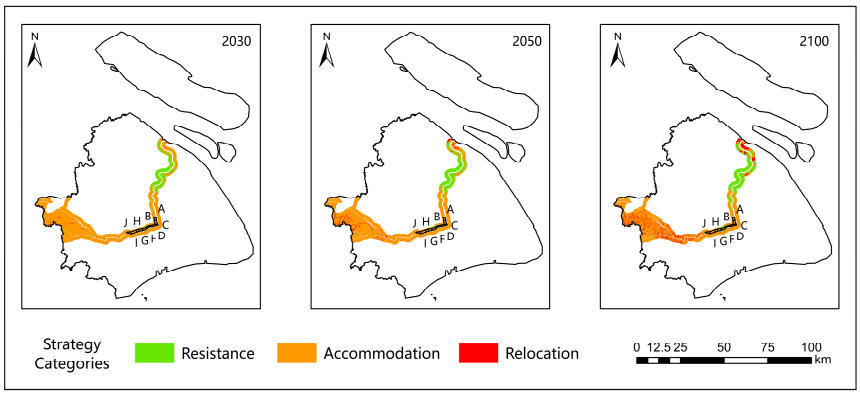

Figure 4. Distribution of the 10 catchment areas and flood risk assessment.

Table 1. Main strategy for adapting to floods in various catchment areas under the background of climate change.

Primary Catchment	2035 Land Use Guidelines	2030 Land Use Strategy	2050 Land Use Strategy	2100 Land Use Strategy
A	Built-up areas	Flood resistance	Flood resistance	Flood accommodation
B	Built-up areas	Flood accommodation	Flood accommodation	Flood resistance
C	Preserved green zones	Flood accommodation	Flood accommodation	Flood accommodation
D	Transitional areas	Flood resistance	Flood resistance	Flood resistance
E	Built-up areas	Flood resistance	Flood resistance	Flood resistance
F	Built-up areas	Flood resistance	Flood resistance	Flood resistance
G	Transitional areas	Flood resistance	Flood resistance	Flood resistance
H	Transitional areas	Flood resistance	Flood resistance	Flood resistance
I	Transitional areas	Flood accommodation	Flood accommodation	Managed inundation
J	Preserved green zones	Flood accommodation	Managed inundation	Managed inundation

4.1. Comparison of Gray-Only Infrastructure and Full BGGI Scenario for Flood Management

Gray-Only Infrastructure of the 10 Sample Catchment Areas (A to J)

Survey data from 2016 was used for the analysis of 10 sample plots, with modifications made to plot A in 2018. For catchment area A, the digital water network was first extracted using GIS, revealing a relatively uniformly distributed drainage pattern (Figure 5), which served as the foundation for further catchment delineation. The delineation results for primary and secondary catchments before modification are shown in the figure, where catchment divisions were mapped and integrated with the existing drainage network. Similarly, GIS calculations were conducted for the other sample plots, and the resulting digital water network extractions are provided in Appendix A (Figures A1–A9).

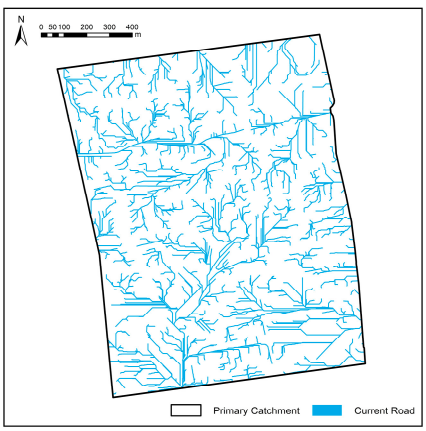

Figure 5. Sample catchment Area A: digital water network extraction results.

After extracting the area elements, the land area is occupied by each feature and the results are listed in Table 2 and illustrated in Figures 6–8.

Table 2. The area and proportion of various features in plot A by the second-level catchment area.

Secondary Catchment Area ID	Catchment Area (m^2)	Water Surface (m^2)	Building Area (m^2)	Road Area (m^2)	Farmland and Green Space (m^2)
1	8017.00	0.00	114.00	58.00	7845.00
2	12,123.00	0.00	107.00	0.00	12,016.00
3	11,400.00	0.00	1333.00	538.00	9529.00
4	33,805.00	2128.00	7140.00	0.00	24,537.00
5	40,469.00	0.00	14.00	835.00	39,620.00
6	27,058.00	1393.00	9281.00	0.00	16,384.00
7	9077.00	0.00	973.00	938.00	7166.00
8	56,389.00	0.00	4878.00	5686.00	45,825.00
9	61,124.00	979.00	15,426.00	7361.00	37,358.00
10	13,428.00	1663.00	3365.00	4189.00	4211.00
11	146,993.00	12,071.00	11,698.00	18,931.00	104,293.00
12	7971.00	0.00	1898.00	2599.00	3474.00
13	37,954.00	0.00	8132.00	8713.00	21,109.00
14	7926.00	0.00	1447.00	3055.00	3424.00
15	320,557.00	13,399.00	73,362.00	33,431.00	200,365.00
16	24,360.00	0.00	6547.00	5116.00	12,697.00
17	16,456.00	0.00	4719.00	5265.00	6472.00
18	15,530.00	0.00	3121.00	4296.00	8113.00
19	16,652.00	0.00	3573.00	4966.00	8113.00
20	40,738.00	0.00	11,902.00	2427.00	26,409.00
21	12,796.00	0.00	2985.00	283.00	9528.00
22	134,278.00	2658.00	39,677.00	7521.00	84,422.00
23	51,087.00	3028.00	5901.00	1264.00	40,894.00
24	29,923.00	0.00	2567.00	1082.00	26,274.00
25	10,000.00	0.00	3877.00	407.00	5716.00
26	8820.00	0.00	3375.00	913.00	4532.00
27	498,607.00	8430.00	98,477.00	79,349.00	312,351.00
Total	1,653,538.00	45,749.00	325,889.00	199,223.00	1,082,677.00
Area Proportion	100.00%	2.77%	19.71%	12.05%	65.48%

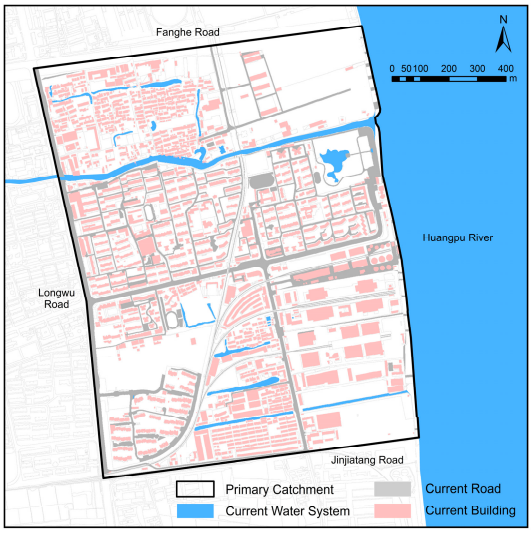

Figure 6. Primary system of catchment area A.

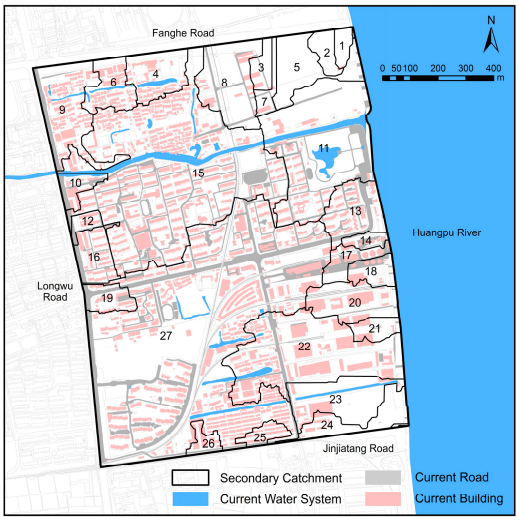

Figure 7. Secondary system of 30 sub-catchment areas of catchment area A.

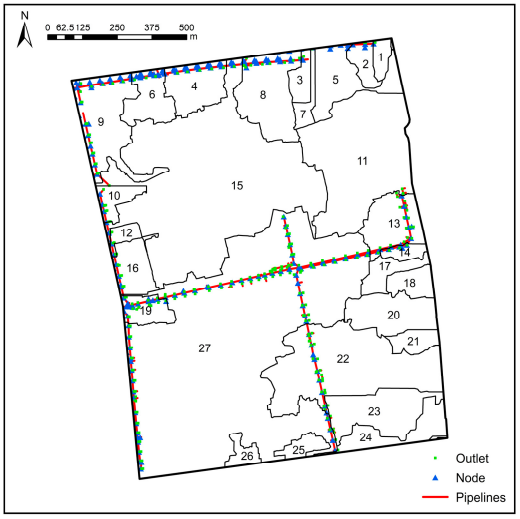

Figure 8. Drainage network in the secondary catchment of plot A.

After calculating the 10 primary catchment areas, total 17,490,699.00 m^2, with an average of 1,749,069.90 m^2. The water surface ratio (percentage of the catchment area occupied by water surfaces) and impervious surface ratio (percentage of the catchment area occupied by buildings and paved roads) were calculated for each plot. The results are shown in Table 3.

Across the 10 primary catchment areas, a total of 217 secondary catchment areas were designated, with areas ranging from 5261 m^2 to 2,016,026 m^2. The average area of a secondary catchment is 80,602 m^2, with a median of 25,424 m^2. Among the 217 secondary catchments, 20 (9.21%) are under 10,000 m^2; 165 (76.03%) range from 10,000 m^2 to 100,000 m^2; 31 (14.29%) range from 100,000 m^2 to 1,000,000 m^2; and one (0.04%) is over 1,000,000 m^2.

This analysis indicates that the waterfront regions are measured in units of tens, hundreds, or thousands of hectares (hm^2). The median water surface ratio is 8.20%, with an average water surface ratio of 7.51%. See Table 4 for details.

For catchment area C, the difference between the pre-drainage water level and ground elevation was set to 1.39 m. The design storage volume and design rainfall for the secondary catchments are shown in Table 5.

In catchment area C, the water surface ratio is 14.05%, with design rainfall for secondary catchments (areas 1 to 22) ranging from 0 mm to 737 mm. GIS calculations indicate an overall design storage volume of 465,534.09 m^3 for plot C.

Table 3. The area and proportions of various features in the 9 sample plots by primary catchment areas.

Primary Catchment Area ID	Catchment Area (m^2)	Water Surface (m^2)	Water Surface Ratio (%)	Building Area (m^2)	Road Area (m^2)	Impervious Surface Ratio (%)	Farmland and Green Space (m^2)
A	1,653,538.00	45,749.00	2.77%	325,889.00	199,223.00	31.76%	1,082,677.00
B	2,229,818.00	184,945.00	8.29%	289,617.00	97,424.00	17.36%	1,657,832.00
C	1,992,578.00	279,906.00	14.05%	63,430.00	92,345.00	7.82%	1,556,897.00
D	1,035,565.00	115,781.00	11.18%	109,892.00	83,625.00	18.69%	726,267.00
E	722,058.00	37,720.00	5.22%	206,820.00	85,642.00	40.50%	391,876.00
F	1,968,550.00	58,295.00	2.96%	498,221.00	199,723.00	35.45%	1,212,311.00
G	1,864,072.00	45,519.00	2.44%	517,851.00	232,470.00	40.25%	1,068,232.00
H	1,393,113.00	131,015.00	9.40%	287,223.00	83,190.00	26.59%	891,685.00
I	3,047,593.00	321,099.00	10.54%	359,513.00	133,394.00	16.17%	2,233,587.00
J	1,583,814.00	129,859.00	8.20%	152,685.00	123,115.00	17.41%	1,178,155.00
Total	17,490,699.00	1,349,888.00	/	2,811,141.00	1,330,151.00	/	11,999,519.00
Area Ratio	100.00%	7.72%	/	16.07%	7.60%	/	68.61%

Table 4. List of the size and scope of the secondary catchment areas.

Area (S) Range (m^2)	<10,000	10,000 ≤ S < 100,000	100,000 ≤ S < 1,000,000	1,000,000 ≤ S
Amount	20	162	33	1
Ratio	9.26%	75.00%	15.28%	0.46%
Average Area (m^2)	8176.55	30,696.43	313,282.45	2,016,026
Median Area (m^2)	8393.00	22,931.00	247,770.00	2,016,026
Average Water Surface	13.28%	12.11%	7.16%	5.97%
Median Water Surface Ratio	1.58%	6.85%	7.29%	5.97%

Table 5. Design regulated storage volume and design rainfall of each secondary catchment area of plot A.

Secondary Catchment Area ID	Secondary Catchment Area (m^2)	Designed Retention Capacity (m^3)	Designed Rainfall Depth (mm)	Secondary Catchment Area ID	Secondary Catchment Area (m^2)	Designed Retention Capacity (m^3)	Designed Rainfall Depth (mm)
1	191,117	28,366.8	148	12	180,085	26,634.3	148
2	46,648	10,231.65	219	13	14,634	2646.6	181
3	44,841	2465.1	55	14	16,263	2164.8	133
4	54,857	28,891.5	527	15	247,770	73,990.95	299
5	15,759	8787.9	558	16	14,468	1047.75	72
6	8133	5997.75	737	17	78,310	17,775.45	227
7	42,315	19,247.25	455	18	648,586	163,571.1	252
8	41,257	7517.4	182	19	11,400	3281.85	288
9	22,381	4227.3	189	20	10,230	3722.4	364
10	205,958	30,412.8	148	21	63,717	15,835.05	249
11	16,968	0	0	22	16,881	5029.2	298

4.2. Result of Surface Water Rate and Flood Adaptability Assessments

4.2.1. Flood Adaptation Model Calculations for Primary Catchment Area Spatial Optimization

After considering the runoff capacity of gray infrastructure in each catchment area, the required increase in water surface ratio for flood retention was calculated in Table 6 and the comparisons between samples are shown in Figure 9.

Table 6. The combined risk of storm surges leads to an increase in flood volume and flood accommodation water surface rate.

Sample ID	Primary Catchment Area (m^2)	Current Water Surface Ratio (%)	2030 Storm Surge-Induced Flood Volume (m^3)	2030 Designed Increase in Water Surface Ratio (%)	2050 Storm Surge-Induced Flood Volume (m^3)	2050 Designed Increase in Water Surface Ratio (%)	2100 Storm Surge-Induced Flood Volume (m^3)	2100 Designed Increase in Water Surface Ratio (%)
A	1,653,538	2.77	164,879.50	No Increase	198,079.81	No Increase	787,175.61	15.56
B	2,229,818	8.29	176,191.30	No Increase	210,200.66	No Increase	1,056,979.88	23.02
C	1,992,578	0.08	108,113.58	2.29	591,427.06	12.88	1,635,216.64	22.88
D	1,035,565	0.16	22,523.09	0.79	262,377.34	10.91	738,161.77	20.06
E	722,058	0.22	239.80	No Increase	255,584.60	15.23	519,234.20	15.94
F	1,968,550	0.08	6862.60	No Increase	343,486.11	7.54	1,369,769.31	22.77
G	1,864,072	0.09	12.59	No Increase	410,868.94	9.54	1,340,034.42	21.77
H	1,393,113	0.12	160.73	No Increase	638,421.96	19.90	999,242.56	11.31
I	3,047,593	0.05	3879.04	No Increase	1,813,001.52	25.93	2,959,639.16	16.43
J	1,583,814	0.10	1116.20	No Increase	948,263.68	26.04	1,876,365.63	25.59

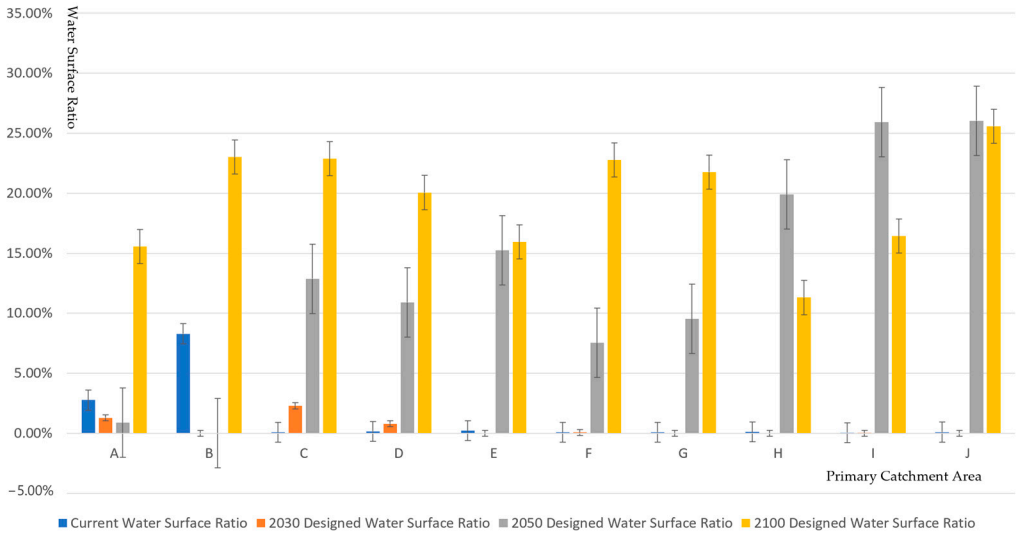

Figure 9. Increased water surface rate for flood accommodation design under combined storm surge risk.

4.2.2. Flood Adaptation Model Calculations for Risk Control in Secondary Catchment Areas

The preceding analysis examined the water surface ratio at the mesoscale of the primary catchment areas along the Huangpu River waterfront and proposed directions for its adjustment. Following the determination of flood adaptation strategies for the primary catchment areas and the design of water surface ratios based on projected future flood volumes under climate change scenarios, it is necessary to further refine flood adaptability through scale transmission. This involves evaluating the differences in water surface ratios between the blue spaces in secondary catchment areas and the overall water surface ratio of the primary catchment areas, as well as making adjustments to the design accordingly.

An assessment of water surface ratios and the proportion of impervious surfaces in secondary catchment areas of varying sizes reveals trends in the water surface ratio changes for secondary catchment areas, as shown in Figure 10.

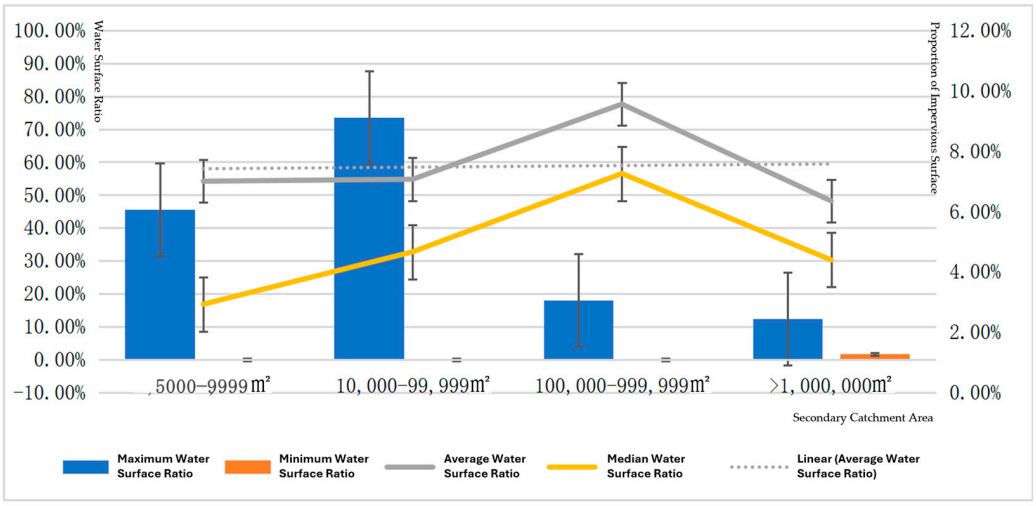

Figure 10. The change trend in water surface rate in the secondary catchment area.

The 217 secondary catchment areas were categorized into four size intervals: 5000–9999 m^2, 10,000–99,999 m^2, 100,000–999,999 m^2, and above 1,000,000 m^2. The average water surface ratio ranged from 6.35% to 9.56%, with the median water surface ratio increasing from 2.92% to 7.26%. The analysis indicates a positive trend where larger secondary catchment areas tend to have higher water surface ratios.

Additionally, impervious surface ratios were calculated by combining the areas of paved roads and building footprints. The trend in changes to impervious surface ratios is shown in Figure 11.

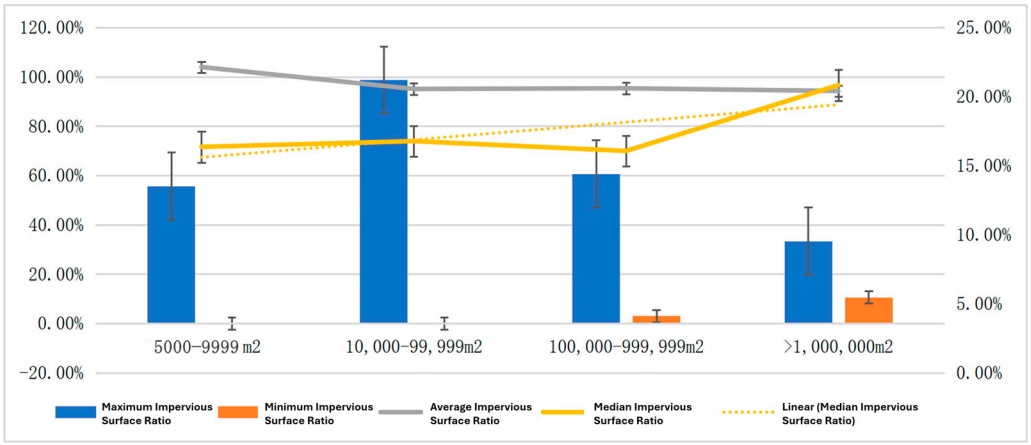

Figure 11. Trend in impervious rate in the secondary catchment area.

Within the same four size intervals mentioned above, the average impervious surface ratio of the secondary catchment areas decreased from 22.13% to 20.40%. The median impervious surface ratio ranged from 16.06% to 20.82%. The trend indicates that larger secondary catchment areas tend to have lower average impervious surface ratios, although the median impervious surface ratio shows a slight increase.

5. Discussion

This study evaluated the effectiveness of coupled blue–green–gray infrastructure (BGGI) in enhancing urban flood resilience in the plain river network region of Minhang District, Shanghai. By integrating natural and engineered solutions, BGGI offers a comprehensive approach to flood management that not only mitigates flood risks but also provides ecological, economic, and social co-benefits. This chapter summarizes the key

findings, discusses the implications for urban planning and policy, and suggests directions for future research.

5.1. Discuss and Compare the Findings

5.1.1. Discussion on Primary Catchment Areas: Water Surface Ratios and Adaptation Strategies

The water surface ratios calculated for the 10 primary catchment areas were analyzed to evaluate their feasibility in achieving flood resilience under future climate change scenarios.

1. Flood Resilience Feasibility of Current Water Surface Ratios: The designed water surface ratios represent idealized scales for achieving resilient flood accommodation. These ratios were assessed under flood scenarios for 2030, 2050, and 2100. If no increase in water surface ratio is recommended for a specific year, it implies that maintaining the current ratio is sufficient for achieving flood resilience.
2. Implications of Increased Water Surface Ratios: For catchment areas where resilience cannot be achieved without increasing the water surface ratio, adjustments must be made prior to the target year. If it is not feasible to meet the designed ratio, alternative flood adaptation strategies—such as flood resistance (e.g., gray infrastructure) or flood accommodation (e.g., controlled inundation)—are necessary.
3. Land Use Adjustments: The magnitude of the required increase in water surface ratio informs land-use planning, ensuring compatibility across developed areas, newly developed zones, and ecological land. This alignment avoids costly mismatches in land functionality.
4. High-Risk Catchments and Recommended Adjustments: Catchment Areas C, E, and J are projected to face significant flood risks by 2100, with water surface ratio increases exceeding 5% needed to ensure resilience. These sites are currently designated as industrial development zones, posing risks of severe damage to life and property under future climate scenarios. Development intensity should be controlled, and these sites should be reclassified as ecological reserves. In contrast, sites A, G, H, and I are at lower risk, requiring no increase in water surface ratio to achieve resilience by 2100. Overall, ecological sites (G, H, I) exhibit better adaptability to future flood risk than development-oriented sites (E, J).

After establishing these water surface ratios, future waterfront development must consider the compounded risks of sea-level rise, land subsidence, and storm surges. The adjusted water surface ratios should guide construction and landscape design to integrate flood retention and aesthetic considerations. For instance, site C must increase its water surface ratio from 7.00% to 12.28% by 2100; site E requires an increase from 2.33% to 7.76% by 2100; and site J must increase its ratio from 3.00% to 8.02% by 2100.

Adaptation strategies for high-density population zones should also be considered. Sites B, D, and E are located in high-density population areas and do not require increased water surface ratios for flood resilience based on current calculations. However, these sites are classified as flood-resistant zones due to localized flooding risks within secondary catchments. Even in low overall flood risk conditions, the heterogeneity of secondary catchments can lead to local inundation, disrupting normal life and threatening safety. As such, these high-density zones prioritize flood resistance strategies, focusing on expanding gray infrastructure, such as underground water storage facilities, to address localized flood risks.

Based on these analyses of water surface ratios across the 10 primary catchment areas, the results provide insights into flood resilience and land-use planning under climate change.

Site A is suitable for development under future climate conditions. The construction of an artificial lake increased the water surface ratio to 26.28%, significantly exceeding the required capacity to accommodate storm surge-induced flooding.

As a built-up area with a population density exceeding 200 people per hectare, site B does not require an increase in its water surface ratio. However, localized flooding within secondary catchments necessitates a flood resistance strategy, including gray infrastructure enhancements such as underground storage systems.

Site C, designated for ecological restoration, requires increases in water surface ratios of 3.27% by 2050 and 5.28% by 2100 to address future flood risks. With low population density, the site is recommended for managed inundation and potential population relocation.

Site D, a built-up residential area, requires a 1.85% increase in water surface ratio to meet 2100 flood retention goals. Retrofitting to accommodate this increase poses challenges for urban renewal and requires flood resistance strategies involving expanded gray infrastructure.

Designated as an industrial development zone, site E requires increases of 0.37% in water surface ratios by 2050 and 5.43% by 2100. However, high flood risks and low population density suggest reclassifying the site as an ecological restoration zone.

These ecological restoration zones have excellent flood resilience, requiring no additional water surface ratio increases by 2050 or 2100. They are also suitable for low-density development, such as industrial bases, while maintaining flood adaptability.

Site J, planned as an industrial zone, requires water surface ratio increases of 1.61% by 2050 and 5.02% by 2100. Due to high flood risks and low population density, the site should undergo careful flood risk assessment and potential reclassification as an ecological reserve.

The study underscores the importance of designing water surface ratios to align with flood retention needs, avoiding costly functional mismatches. At the primary catchment level, these ratios support future land-use planning, while at the secondary catchment level, they inform localized interventions to enhance flood resilience. This multi-scale approach provides critical guidance for integrating climate adaptation and land-use strategies in waterfront zones such as the Huangpu River.

5.1.2. Analysis of Secondary Catchment Areas: Water Surface Ratios and Adaptation Measures

The analysis of secondary catchment areas reveals that those with low or zero water surface ratios can benefit from strategic integration with neighboring areas within the same primary catchment. By coordinating their capacities through integrated design approaches—such as utilizing pipeline networks for inter-area drainage—these catchments can more effectively achieve flood retention objectives. Of the 217 secondary catchment areas analyzed, 63 were found to have a water surface ratio of zero, accounting for 18% of the total. These areas lack sufficient capacity to manage surface runoff independently and require interventions to prevent additional drainage burdens on external systems.

To enhance flood retention capacity, secondary catchments with zero or minimal water surface ratios may implement measures such as increasing their water surface ratio or adopting sponge-city techniques like recessed green spaces. However, uniformly lowering the elevations of green spaces or agricultural land to function as sponges is often infeasible due to variations in land use rights and ownership. Conversely, raising impervious surfaces such as roads or buildings to increase retention capacity is also challenging.

For instance, in catchment area E, secondary catchments 5, 9, and 10 currently have a water surface ratio of zero. To meet the retention requirements for 2050 and 2100, adjustments to green spaces and agricultural land would be necessary. By 2050, catchments 5, 9, and 10 would need reductions in elevation of 1.8 cm, 16.8 cm, and 0.3 cm, respectively. For 2100, the reductions would increase significantly to 96.0 cm, 57.7 cm, and 72.8 cm. These

adjustments are calculated to meet the projected water surface ratios for each respective year, including 0.4%, 5.72%, and 0.08% for 2050, and 20.72%, 19.55%, and 19.65% for 2100.

The primary objective of increasing water surface ratios is to expand flood retention volume, which does not necessarily require permanent water coverage. Instead, the focus is on creating dynamic water surfaces capable of accommodating runoff during extreme flood events. Given the challenges associated with large-scale elevation modifications, a more practical approach involves localized land adjustments to increase water surface ratios. Rather than uniformly lowering or raising land elevation, partial modifications within secondary catchments offer greater flexibility and site-specific solutions. This strategy aligns with the broader goal of achieving on-site surface runoff absorption without over-reliance on external drainage systems.

By prioritizing site-specific, adaptable interventions, secondary catchment areas can play a critical role in enhancing flood retention capacity under future climate scenarios. These measures offer a feasible approach to integrating hydrological performance with existing land use and ownership structures, supporting sustainable flood management.

Under the context of climate change, compounded factors such as storm surges are projected to cause progressively increasing extreme flood volumes by 2030, 2050, and 2100. Based on calculations using the same methodology applied earlier for 2030's extreme flood volumes, it was determined that 36 out of 217 secondary catchment areas lack sufficient retention capacity to meet flood accommodation requirements. The current water surface ratios for these catchments fall below the designed ratios needed to achieve flood resilience, necessitating targeted increases in water surface ratios. The specific requirements for increasing water surface ratios are summarized in Table 7.

Table 7. List of secondary catchment areas with current water surface ratio less than design water surface ratio in 2030.

Primary Catchment Area	Secondary Catchment Area ID	Current Water Surface Ratio (%)	Designed Increase in Water Surface Ratio (%)	Primary Catchment Area	Secondary Catchment Area ID	Current Water Surface Ratio (%)	Designed Increase in Water Surface Ratio (%)	Primary Catchment Area	Secondary Catchment Area ID	Current Water Surface Ratio (%)	Designed Increase in Water Surface Ratio (%)
A	1	0.00%	873.36	A	22	197.95	471.98	B	13	458.73	600.84
A	2	0.00%	873.36	A	23	592.71	215.94	B	15	268.25	449.44
A	3	0.00%	771.74	A	24	0.00%	873.36	B	16	680.26	57.63
A	5	0.00%	873.36	A	25	0.00%	474.41	B	18	653.55	463.47
A	7	0.00%	770.40	A	27	169.07	12.19	C	1	899.55	16.97
A	8	0.00%	630.94	B	2	0.00%	1212.12	C	3	333.18	633.30
A	13	0.00%	873.36	B	4	0.00%	1212.12	C	11	0.00%	648.79
A	14	0.00%	873.36	B	5	42.62%	1169.50	D	13	0.00%	269.94
A	17	0.00%	873.36	B	6	0.00%	1212.12	D	14	109.35	239.99
A	18	0.00%	873.36	B	8	0.00%	1212.12	D	15	9.19%	206.76
A	20	0.00%	873.36	B	10	0.00%	1212.12	E	14	13.03%	21.62%
A	21	0.00%	873.36	B	12	139.29	1072.83	G	24	0.00%	0.97%

Based on calculations for extreme flood volumes projected for 2050 under compounded factors such as storm surges, 147 out of 217 secondary catchment areas were found to lack sufficient retention capacity to meet flood accommodation requirements. The current water surface ratios in these catchments fall below the designed ratios necessary for flood resilience, indicating the need for targeted increases in water surface ratios. The specific requirements for these adjustments are summarized in Table 8.

Based on calculations for extreme flood volumes projected for 2100, driven by compounded factors such as storm surges, 211 out of 217 secondary catchment areas were found to lack sufficient retention capacity to meet flood accommodation requirements. The current water surface ratios in these catchments fall short of the designed ratios necessary

for achieving flood resilience, necessitating specific increases in water surface ratios. The detailed requirements for these adjustments are summarized in Table 9.

Table 8. List of secondary catchment areas with current water surface ratio less than designed water surface ratio in 2050.

Primary Catchment Area	Secondary Catchment Area ID	Current Water Surface Ratio (%)	Designed Increase in Water Surface Ratio (%)	Primary Catchment Area	Secondary Catchment Area ID	Current Water Surface Ratio (%)	Designed Increase in Water Surface Ratio (%)	Primary Catchment Area	Secondary Catchment Area ID	Current Water Surface Ratio (%)	Designed Increase in Water Surface Ratio (%)
A	1	0.00	17.47	D	10	7.38	14.50	G	21	3.41	23.75
A	2	0.00	8.80	D	11	0.00	18.02	G	22	0.00	26.20
A	11	8.21	3.40	D	12	4.60	7.53	G	23	0.29	25.99
A	13	0.00	17.37	D	13	0.00	26.20	G	24	0.00	26.20
A	14	0.00	17.47	D	14	1.09	25.41	G	25	2.35	6.50
A	15	4.18	0.00	D	15	0.09	26.13	H	1	0.00	22.80
A	16	0.00	0.00	D	16	0.81	25.62	H	2	0.00	24.30
A	17	0.00	17.47	D	17	12.91	7.21	H	3	7.87	7.52
A	18	0.00	17.47	E	1	1.70	10.15	H	4	0.00	24.42
A	20	0.00	13.82	E	2	10.71	9.25	H	6	7.67	18.58
A	21	0.00	17.47	E	3	11.86	16.62	H	8	0.00	23.06
A	22	1.98	2.70	E	6	3.21	11.62	H	9	19.53	8.57
A	23	5.93	9.24	E	8	1.78	20.95	H	10	14.96	12.61
A	24	0.00	11.97	E	9	8.97	1.70	H	11	0.00	25.84
B	2	0.00	31.64	E	10	2.34	15.59	H	12	17.91	13.29
B	4	0.00	18.28	E	11	0.35	25.66	H	13	5.15	9.07
B	5	0.43	16.23	E	12	0.61	25.76	H	15	4.00	20.45
B	6	0.00	15.08	E	13	5.00	8.80	H	16	0.00	26.07
B	8	0.00	15.08	E	14	0.13	26.11	H	18	0.02	26.19
B	10	0.00	6.35	E	15	20.43	11.48	I	1	1.97	24.78
B	12	1.39	2.46	F	5	2.05	8.92	I	2	3.16	23.93
B	13	4.59	11.41	F	7	5.12	22.51	I	4	18.08	12.96
B	15	2.68	13.30	F	8	12.19	7.19	I	7	7.51	20.79
B	16	6.80	29.56	F	9	17.66	12.41	I	10	5.43	22.29
B	17	8.74	25.81	F	10	15.38	14.31	I	11	33.55	2.03
B	18	6.54	23.23	F	11	13.57	16.42	I	12	33.64	1.96
B	20	11.97	10.39	F	12	1.72	10.86	I	13	20.28	11.59
C	1	9.00	17.72	F	13	14.94	15.44	I	15	2.04	24.73
C	2	13.29	0.00	F	15	6.96	21.19	I	17	5.97	21.57
C	3	3.33	23.80	F	16	0.17	12.95	I	20	16.69	14.17
C	4	31.92	3.20	F	17	0.10	16.38	J	1	5.01	22.59
C	5	33.80	1.85	F	18	0.17	26.08	J	2	3.24	23.87
C	6	44.69	0.00	F	19	0.25	26.02	J	3	7.03	21.14
C	7	27.57	6.34	F	20	0.22	8.99	J	4	34.76	1.07
C	8	11.04	18.24	F	21	1.19	15.76	J	5	19.13	12.42
C	9	11.45	17.95	F	22	14.11	12.72	J	6	15.71	14.88
C	10	8.95	13.25	F	23	2.10	21.02	J	7	9.87	19.09
C	11	0.00	17.34	F	24	9.18	19.59	J	9	0.00	26.20
C	12	8.96	1.04	F	25	0.64	0.70	J	10	13.57	16.42
C	15	18.10	5.77	G	3	0.00	0.06	J	11	12.11	17.48
C	16	4.39	22.71	G	4	0.00	1.61	J	12	6.90	21.23
C	17	13.76	12.54	G	13	4.84	12.56	J	13	7.29	20.94
C	20	22.05	7.61	G	14	3.44	23.72	J	14	12.77	17.00
C	21	15.06	8.07	G	15	9.82	19.13	J	15	3.37	23.77
C	22	18.06	13.19	G	16	21.35	6.17	J	16	10.03	18.98
D	6	10.34	18.75	G	17	0.32	25.97	J	17	5.66	22.12
D	7	12.75	4.50	G	18	0.38	14.22	J	18	1.61	24.85
D	8	12.81	16.59	G	19	0.00	26.20	J	19	8.14	18.83
D	9	4.59	21.41	G	20	0.57	25.79	J	20	0.00	22.61

The data presented above show that as time progresses, the number of secondary catchment areas unable to accommodate flood volumes increases, and the gap between the current water surface ratios and the designed ratios widens. Determining which year's designed water surface ratio should serve as the baseline for flood adaptation construction depends on factors such as urban–rural planning priorities, land ownership structures, and construction costs. For adjustments made in 2020, if the goal is to achieve flood resilience for

the next 30 years, the 2050 designed water surface ratio should be adopted. Alternatively, if the target is flood resilience over an 80-year horizon, the 2100 designed ratio should be used. However, it is essential to note that as the adaptation target extends further into the future under climate change, the scale of necessary site modifications increases, along with the associated construction costs. As indicated in the multi-indicator evaluation framework discussed in the previous chapter, when the designed water surface ratio reaches a certain threshold and exceeds critical evaluation standards, the flood adaptation strategy may need to shift from flood accommodation to managed inundation. This highlights the importance of balancing ambitious flood resilience targets with practical and economic considerations.

Table 9. List of secondary catchment areas with current water surface ratio less than designed water surface ratio in 2100.

Primary Catchment Area	Secondary Catchment Area ID	Current Water Surface Ratio (%)	Designed Increase in Water Surface Ratio (%)	Primary Catchment Area	Secondary Catchment Area ID	Current Water Surface Ratio (%)	Designed Increase in Water Surface Ratio (%)	Primary Catchment Area	Secondary Catchment Area ID	Current Water Surface Ratio (%)	Designed Increase in Water Surface Ratio (%)
A	1	0.00	26.20	C	21	15.06	28.86	G	13	4.84	21.40
A	2	0.00	34.86	C	22	18.06	26.20	G	14	3.44	26.20
A	3	0.00	12.53	D	1	16.79	16.34	G	15	9.82	26.20
A	4	6.29	0.03	D	2	13.37	18.34	G	16	21.35	7.83
A	5	0.00	47.00	D	3	20.72	18.34	G	17	0.32	26.20
A	6	5.15	0.10	D	4	31.33	27.80	G	18	0.38	24.43
A	7	0.00	33.88	D	5	12.42	15.83	G	19	0.00	26.20
A	9	1.60	0.28	D	6	10.34	26.20	G	20	0.57	26.20
A	10	12.38	1.35	D	7	12.75	21.48	G	21	3.41	26.20
A	11	8.21	39.73	D	8	12.81	26.58	G	22	0.00	26.20
A	12	0.00	9.20	D	9	4.59	27.69	G	23	0.29	26.20
A	13	0.00	26.30	D	10	7.38	30.50	G	24	0.00	17.01
A	14	0.00	26.20	D	11	0.00	29.71	G	25	2.35	20.04
A	15	4.18	4.09	D	12	4.60	26.22	H	3	7.87	9.04
A	16	0.00	9.20	D	13	0.00	26.20	H	5	29.23	22.28
A	17	0.00	26.20	D	14	1.09	26.20	H	7	25.32	12.15
A	18	0.00	26.20	D	15	0.09	26.20	H	9	19.53	5.66
A	19	0.00	9.20	D	16	0.81	26.20	H	10	14.96	12.11
A	20	0.00	29.85	D	17	12.91	13.43	H	11	0.00	23.64
A	21	0.00	22.62	E	1	1.70	5.09	H	12	17.91	24.21
A	22	1.98	20.12	E	2	10.71	25.02	H	13	5.15	17.08
A	23	5.93	11.28	E	3	11.86	16.82	H	14	51.93	26.20
A	24	0.00	18.39	E	4	9.77	1.53	H	15	4.00	6.90
A	25	0.00	18.50	E	6	3.21	3.86	H	16	0.00	26.33
A	26	0.00	8.87	E	7	21.47	1.19	H	17	44.60	26.20
A	27	1.69	14.96	E	8	1.78	27.34	H	18	0.02	26.20
B	1	0.00	19.00	E	10	2.34	16.14	H	19	53.24	26.20
B	2	0.00	31.80	E	11	0.35	26.46	H	20	45.94	26.20
B	3	0.00	22.09	E	12	0.61	26.20	I	1	1.97	8.68
B	4	0.00	46.73	E	13	5.00	22.66	I	2	3.16	25.29
B	5	0.43	6.63	E	14	0.13	26.20	I	3	81.82	26.20
B	6	0.00	54.03	E	15	20.43	26.20	I	4	18.08	25.83
B	7	5.25	23.27	F	1	6.03	0.48	I	5	76.82	26.08
B	8	0.00	57.65	F	2	15.11	0.53	I	6	53.22	26.19
B	9	11.96	23.27	F	3	4.38	3.60	I	7	7.51	3.16
B	10	0.00	66.38	F	4	13.76	14.04	I	8	42.73	26.20
B	11	5.57	23.44	F	5	2.05	23.85	I	9	51.16	26.20
B	12	1.39	31.51	F	6	7.57	21.72	I	10	5.43	26.20
B	13	4.59	39.11	F	7	5.12	26.20	I	11	33.55	26.20
B	14	7.56	17.98	F	8	12.19	36.26	I	12	33.64	26.20
B	15	2.68	55.21	F	9	17.66	27.26	I	13	20.28	26.20
B	16	6.80	36.36	F	10	15.38	27.00	I	14	65.67	26.20
B	17	8.74	38.19	F	11	13.57	26.20	I	15	2.04	13.40
B	18	6.54	38.73	F	12	1.72	22.68	I	16	55.67	26.20
B	19	10.63	22.46	F	13	14.94	26.20	I	17	5.97	16.37

Table 9. *Cont.*

Primary Catchment Area	Secondary Catchment Area ID	Current Water Surface Ratio (%)	Designed Increase in Water Surface Ratio (%)	Primary Catchment Area	Secondary Catchment Area ID	Current Water Surface Ratio (%)	Designed Increase in Water Surface Ratio (%)	Primary Catchment Area	Secondary Catchment Area ID	Current Water Surface Ratio (%)	Designed Increase in Water Surface Ratio (%)
B	20	11.97	32.56	F	14	11.55	20.96	I	18	70.50	26.20
B	21	48.43	48.58	F	15	6.96	26.20	I	19	60.34	26.20
B	22	20.56	33.61	F	16	0.17	27.47	I	20	16.69	25.26
B	23	11.49	15.30	F	17	0.10	28.20	I	21	65.35	26.20
B	24	12.30	4.25	F	18	0.17	26.20	J	1	5.01	12.47
C	1	9.00	25.50	F	19	0.25	26.20	J	2	3.24	15.22
C	2	13.29	15.79	F	20	0.22	32.33	J	3	7.03	25.78
C	3	3.33	26.20	F	21	1.19	23.83	J	4	34.76	26.24
C	4	31.92	26.20	F	22	14.11	23.99	J	5	19.13	26.20
C	5	33.80	24.80	F	23	2.10	24.51	J	6	15.71	26.20
C	6	44.69	23.45	F	24	9.18	26.20	J	7	9.87	26.20
C	7	27.57	22.85	F	25	0.64	21.92	J	8	43.16	26.20
C	8	11.04	23.92	G	1	0.99	21.99	J	9	0.00	26.20
C	9	11.45	25.02	G	2	0.00	21.66	J	10	13.57	26.20
C	10	8.95	25.03	G	3	0.00	21.61	J	11	12.11	26.20
C	11	0.00	31.02	G	4	0.00	20.22	J	12	6.90	26.20
C	12	8.96	25.89	G	5	5.89	21.82	J	13	7.29	26.04
C	13	10.96	17.87	G	6	1.46	22.24	J	14	12.77	26.20
C	14	8.07	18.34	G	7	14.85	21.13	J	15	3.37	26.20
C	15	18.10	27.19	G	8	27.16	20.96	J	16	10.03	26.20
C	16	4.39	26.53	G	9	6.52	21.98	J	17	5.66	25.51
C	17	13.76	21.06	G	10	9.46	21.53	J	18	1.61	26.39
C	18	15.28	18.27	G	11	10.73	20.96	J	19	8.14	27.71

5.2. Limitations of the Study

While this study provides valuable insights into the integration of blue–green and gray infrastructure for flood resilience, certain limitations should be acknowledged. The resolution of the DEM data used in hydrological analysis may affect the precision of catchment delineation. While higher-resolution data would enhance accuracy, it may not be universally available across all study areas. Additionally, hydrological modeling relies on the completeness and quality of historical flood data, which can vary by region. Although the findings are specific to the Minhang District in Shanghai, the methodology and key insights remain applicable to other urban regions with similar hydrological and socio-economic conditions.

Predictive climate scenarios for 2030, 2050, and 2100 introduce inherent uncertainties, as they may not fully account for future urbanization trends or unexpected climate variables. While MIKE21 and other hydrological models provide robust simulations, certain simplifications are necessary, which may not fully capture complex interactions such as groundwater–surface water dynamics. Socio-economic considerations, including land ownership, policy implementation, and public acceptance of blue–green infrastructure, represent additional challenges that warrant further investigation.

Despite these limitations, the study contributes to advancing flood resilience strategies by demonstrating the benefits of an integrated blue–green–gray infrastructure approach. Future research should explore higher-resolution data sources, expand analysis to diverse geographic settings, and incorporate dynamic socio-economic and ecological factors to enhance applicability and robustness.

5.3. Future Research Directions

The implementation of BGGI for resilient flood adaptation faces a range of technical, economic, and policy-level challenges. Overcoming these barriers is essential for ensuring the successful execution of projects and advancing effective flood adaptation strategies.

Access to high-quality, comprehensive geographic, hydrological, and meteorological data is essential for developing accurate BGGI models. However, some regions may face data limitations or quality issues, which can compromise the reliability and applicability of these models. Additionally, the interdisciplinary nature of BGGI—spanning hydrology, ecology, and urban planning—adds complexity to model development. Effective integration of expertise across these disciplines is critical for ensuring model accuracy and feasibility, yet presents significant coordination challenges.

Implementing resilient flood adaptation strategies using BGGI often requires substantial financial investment, including infrastructure construction, technological deployment, and ongoing maintenance costs. Inadequate funding can limit the scale and effectiveness of projects, while conflicting interests among stakeholders, such as landowners and developers, may create additional barriers to implementation. Addressing these tensions requires balancing social equity, economic sustainability, and stakeholder interests to ensure successful project outcomes.

Policy and regulatory inconsistencies across different governance levels can further hinder the interdisciplinary collaboration needed for BGGI implementation. Coordinating and integrating policy frameworks ensure effective project execution. Furthermore, a lack of strong policy support for resilient flood adaptation—whether due to insufficient governmental commitment or weak enforcement mechanisms—can impede progress and reduce long-term project viability.

Overcoming these barriers requires a comprehensive, integrated approach. Technical challenges can be mitigated by establishing data-sharing platforms, utilizing open-source modeling tools, and implementing technical training programs to enhance capacity building. Economic obstacles can be addressed by exploring sustainable funding mechanisms, such as public–private partnerships and green financing strategies, to secure the necessary resources for implementation and maintenance. To overcome policy challenges, fostering intergovernmental collaboration and cross-sector policy integration is critical in creating a regulatory environment that supports BGGI resilience strategies.

By systematically addressing technical, economic, and policy challenges, cities can enhance BGGI implementation and develop more effective, resilient flood adaptation strategies. This comprehensive approach ensures that projects can navigate complex barriers while maintaining sustainability and adaptability goals.

This study demonstrates the potential of coupled blue–green–gray infrastructure to transform urban flood management, providing a resilient, sustainable, and cost-effective approach for cities facing increasing climate-related flood risks. Integrating natural and engineered solutions enhances flood resilience, environmental quality, and community well-being, aligning with global sustainability and climate adaptation goals. By adopting BGGI, cities can move toward a future where urban resilience is built into the very fabric of their design, ensuring safe, healthy, and vibrant urban spaces for generations to come.

6. Conclusions

Shanghai, situated within the Jiangnan Plain's river network region, is characterized by minimal variations in elevation. Understanding the distribution and flow direction of runoff across catchment areas is essential for managing flood convergence and preventing uncontrolled inundation. The water surface ratio, particularly in water-dominated regions, is critical in floodwater management. This research examines the water surface ratio as a key determinant of flood adaptation at the mesoscale within flood accommodation zones and offers strategic recommendations for ensuring water security. It provides insights into catchment delineation, water surface ratio calculations, the scaling and morphology of blue spaces, and the theoretical framework supporting these approaches.

Statistical analyses of 10 primary and 217 secondary catchment areas along the Huangpu River indicate that the average size of primary catchments is approximately 4 km^2. In contrast, secondary catchments have a median size of 30,000 m^2 and an average of 110,000 m^2, suggesting that mesoscale waterfront areas typically range from several hectares to hundreds of hectares. Given Shanghai's geographic location on an alluvial plain, maintaining an optimal water surface ratio along the Huangpu River waterfront is critical for flood resilience and water security.

For a specific site, understanding its catchment boundaries and the capacity of its gray infrastructure is essential for calculating runoff retention potential. Catchment delineation serves as a prerequisite for applying hydrological models that compute distributed runoff capacity. This chapter employs the volumetric method to develop a runoff capacity model, analyzing the relationship between runoff retention and flood risk based on variations in surface types and drainage coefficients.

The analysis of the 10 study catchment areas confirms the feasibility of implementing resilient flood accommodation strategies for future flood scenarios. It emphasizes the necessity of determining appropriate water surface ratio scales to enhance flood adaptability. This approach supports tailored water surface ratio adjustments for built-up areas, newly developed zones, and ecological lands, helping to prevent functional mismatches.

The study highlights that catchment area J faces a high risk of flooding in the future. As it is currently designated for industrial development, this could pose severe risks to life and property. Thus, it is recommended that development be restricted in this area and that the catchment be reclassified as an ecological reserve. Conversely, catchment areas G, H, and I exhibit lower flood risks and may be suitable for industrial development under well-regulated planning frameworks.

An analysis of water and impervious surface ratios in secondary catchments reveals a trend wherein larger catchments generally have higher water surface ratios and lower impervious surface ratios. However, for secondary catchments with zero water surface ratios, uniformly lowering the elevation of green spaces and farmland is impractical. To enhance localized flood retention, increasing their water surface ratios is necessary, with a focus on introducing both regulatory and retention water bodies.

From the perspectives of urban planning and landscape architecture, analyzing water surface ratios in primary catchments provides a scientific foundation for calculating gray infrastructure runoff capacity, retention volumes, and optimal water surface ratios. This knowledge informs future planning and construction strategies. Research into secondary catchment water surface ratios further determines whether runoff can be effectively absorbed locally, thereby reducing the need for unnecessary expansion of stormwater networks in tertiary catchments. The delineation of catchment areas and the strategic design of water surface ratios for the Huangpu River waterfront serve as an essential link between macro- and microscale planning. These strategies play a significant role in shaping flood adaptability and ensuring long-term water security in waterfront areas.

Author Contributions: Conceptualization, C.G. and L.Z.; methodology, L.Z.; software, M.W. and R.Z.; validation, L.Z., M.W. and C.G.; formal analysis, L.Z.; investigation, L.Z.; resources, C.G.; data curation, M.W.; writing—original draft preparation, L.Z.; writing—review and editing, L.Z.; visualization, M.W. and R.Z.; supervision, C.G.; project administration, L.Z.; funding acquisition, C.G. and L.Z. All authors have read and agreed to the published version of the manuscript.

Funding: This research received no external funding.

Data Availability Statement: The original contributions presented in this study are included in the article. Further inquiries can be directed to the corresponding author.

Conflicts of Interest: The authors declare no conflicts of interest.

Appendix A

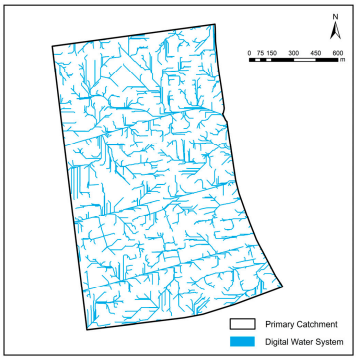

Figure A1. Sample catchment area B: digital water network extraction results.

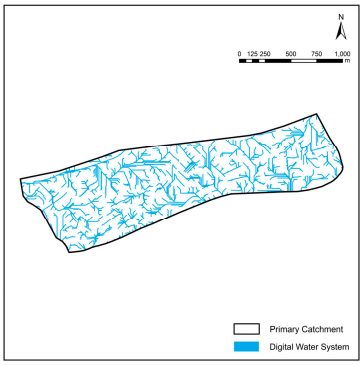

Figure A2. Sample catchment area C: digital water network extraction results.

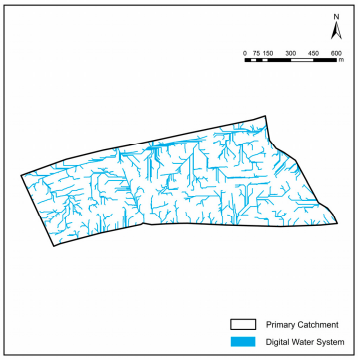

Figure A3. Sample catchment area D: digital water network extraction results.

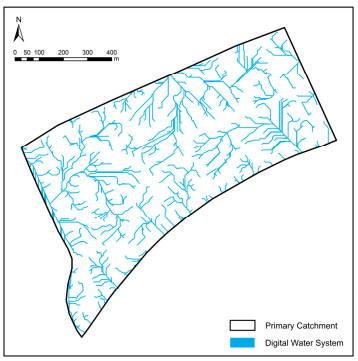

Figure A4. Sample catchment area E: digital water network extraction results.

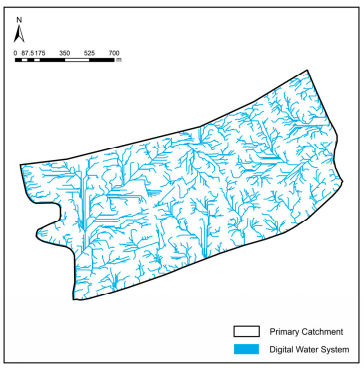

Figure A5. Sample catchment area F: digital water network extraction results.

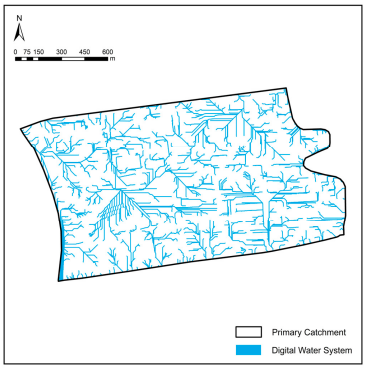

Figure A6. Sample catchment area G: digital water network extraction results.

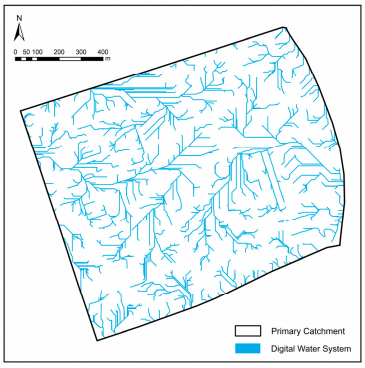

Figure A7. Sample catchment area H: digital water network extraction results.

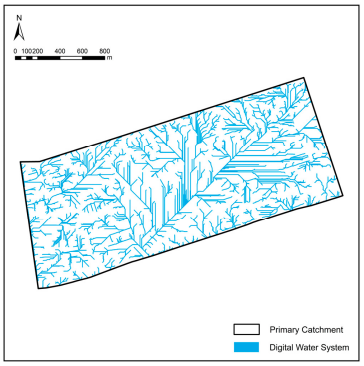

Figure A8. Sample catchment area I: digital water network extraction results.

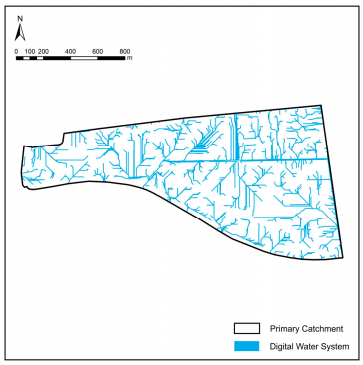

Figure A9. Sample catchment area J: digital water network extraction results.

References

1. Chou, J.; Sun, M.; Dong, W.; Zhao, W.; Li, J.; Li, Y.; Zhou, J. Assessment and Prediction of Climate Risks in Three Major Urban Agglomerations of Eastern China. *Sustainability* **2021**, *13*, 13037. [CrossRef]
2. Lee, H.; Song, K.; Kim, G.; Chon, J. Flood-Adaptive Green Infrastructure Planning for Urban Resilience. *Landsc. Ecol. Eng.* **2021**, *17*, 427–437. [CrossRef]
3. Gupta, A.; De, B. A Systematic Review on Urban Blue-Green Infrastructure in the South Asian Region: Recent Advancements, Applications, and Challenges. *Water Sci. Technol.* **2024**, *89*, 382–403. [CrossRef] [PubMed]
4. Liu, S.; Chan, F.; Chen, W.; Netusil, N.; Feng, M.; Xie, L.; Qi, Y.; Xu, S.; Cheshmehzangi, A. Home-Buying Decisions Influenced by the Implementation of Nature-Based Solutions: The Case of Sponge City, Guiyang SW China. *Nat.-Based Solut.* **2024**, *5*, 100115. [CrossRef]
5. Shen, X.; Ge, M.; Wang, Q.; Padua, M.; Chen, D. Restoring, Remaking and Greening Freshwater Ecosystems: A Review of Projects in China. *Ecol. Restor.* **2022**, *40*, 172–178. [CrossRef]
6. Tiggeloven, T.; de Moel, H.; Ward, P. Towards Holistic Global Coastal Flood Risk Assessments Including Nature-Based Solutions. In Proceedings of the EGU23, the 25th EGU General Assembly, Vienna, Austria, 23–28 April 2023; EGU-17430. [CrossRef]
7. Gallois, L.; van den Homberg, M.; Cinelli, M. Multiple criteria-based assessments of Nature-Based Solutions for flood management: A review. In Proceedings of the EGU23, the 25th EGU General Assembly, Vienna, Austria, 23–28 April 2023; EGU23-9844. [CrossRef]
8. Olanrewaju, O.S.; Lazzaro, U. Review of Nature based Ecohydraulic Aquaforest Technology for Coastal Resilience and Sea Level Rise Climate-Induced Adaptation—Part A. *Preprints* **2023**, 2023050812. [CrossRef]
9. Lee, H.; Kang, Y.; Kim, H.S.; Kim, S.; Kim, K. Analysis of Climate Change Mitigation and Flood Reduction Effects of Nature-based Solutions. In Proceedings of the EGU23, the 25th EGU General Assembly, Vienna, Austria, 23–28 April 2023; EGU23-14527. [CrossRef]
10. Quattrone, G. Green and Blue Infrastructures and Nature-Based Solutions to Reduce Pollutant Emissions and Make Transitioning Urban Ecosystems More Climate Change-Adaptive. *Green Build. Constr. Econ.* **2023**, *4*, 80–89. [CrossRef]
11. Kapetas, L.; Fenner, R. Integrating Blue-Green and Grey Infrastructure through an Adaptation Pathways Approach to Surface Water Flooding. *Philos. Trans. R. Soc. A* **2020**, *378*, 20190204. [CrossRef]
12. Demuzere, M.; Orru, K.; Heidrich, O.; Olazabal, E.; Geneletti, D.; Orru, H.; Bhave, A.G.; Mittal, N.; Feliu, E.; Faehnle, M. Mitigating and Adapting to Climate Change: Multi-Functional and Multi-Scale Assessment of Green Urban Infrastructure. *J. Environ. Manag.* **2014**, *146*, 107–115. [CrossRef]
13. Mugume, S.; Nakyanzi, L. Evaluation of Effectiveness of Blue-Green Infrastructure for Reduction of Pluvial Flooding under Climate Change and Internal System Failure Conditions. *Blue-Green Syst.* **2024**, *6*, 264–292. [CrossRef]
14. Holling, C.S. Resilience and Stability of Ecological Systems. *Annu. Rev. Ecol. Syst.* **1973**, *4*, 1–23. [CrossRef]
15. Peck, A.J.; Adams, S.L.; Armstrong, A.; Bartlett, A.K.; Bortman, M.L.; Branco, A.B.; Brown, M.L.; Donohue, J.L.; Kodis, M.; McCann, M.J.; et al. A New Framework for Flood Adaptation: Introducing the Flood Adaptation Hierarchy. *Ecol. Soc.* **2022**, *27*, 5. [CrossRef]
16. Holling, C.S.; Schindler, D.W.; Walker, B.W.; Roughgarden, J. Biodiversity in the Functioning of Ecosystems: An Ecological Synthesis. In *Biodiversity and Loss: Economic and Ecological Issues*; Perrings, C., Maler, L.G., Folke, C., Holling, C.S., Jansson, B.O., Eds.; Cambridge University Press: Cambridge, UK, 1995; pp. 44–83. [CrossRef]
17. Tyler, S.; Moench, M. A Framework for Urban Climate Resilience. *Clim. Dev.* **2012**, *4*, 311–326. [CrossRef]
18. Jabareen, Y. Planning the Resilient City: Concepts and Strategies for Coping with Climate Change and Environmental Risk. *Cities* **2013**, *31*, 220–229. [CrossRef]

19. Wang, L.; Cui, S.; Li, Y.; Huang, H.; Manandhar, B.; Nitivattananon, V.; Fang, X.; Huang, W. A Review of the Flood Management: From Flood Control to Flood Resilience. *Heliyon* **2022**, *8*, e11763. [CrossRef] [PubMed]
20. Zhu, L.Q. Research on Multi-Level Blue-Green Collaborative Planning Approaches for Estuary City Waterfront Spaces Under the Goal of Flood Adaptation. Ph.D. Thesis, Huazhong Agricultural University, Wuhan, China, 2022.
21. Fenner, R. Editorial: Great Floods Have Flown from Simple Sources. *Philos. Trans. A Math. Phys. Eng. Sci.* **2020**, *378*, 20190199. [CrossRef]
22. Tansar, H.; Duan, H.F.; Mark, O. A Multi-Objective Decision-Making Framework for Implementing Green-Grey Infrastructures to Enhance Urban Drainage System Resilience. *J. Hydrol.* **2023**, *620*, 129381. [CrossRef]
23. Cristiano, E.; ten Veldhuis, M.-C.; van de Giesen, N. Spatial and Temporal Variability of Rainfall and Their Effects on Hydrological Response in Urban Areas—A Review. *Hydrol. Earth Syst. Sci.* **2017**, *21*, 3859–3878. [CrossRef]
24. Wang, J.; Gao, W.; Xu, S.; Yu, L. Evaluation of the Combined Risk of Sea Level Rise, Land Subsidence, and Storm Surges on the Coastal Areas of Shanghai, China. *Clim. Chang.* **2012**, *115*, 537–558. [CrossRef]
25. Yin, J.; Jonkman, S.; Lin, N.; Yu, D.; Aerts, J.; Wilby, R.; Pan, M.; Wood, E.; Bricker, J.; Ke, Q.; et al. Flood Risks in Sinking Delta Cities: Time for a Reevaluation? *Earth's Future* **2020**, *8*, e2020EF001614. [CrossRef]
26. Wang, H.; Cao, Y.; Wu, X.; Zhao, A.; Xie, Y. Estimation and Potential Analysis of Land Population Carrying Capacity in Shanghai Metropolis. *Int. J. Environ. Res. Public Health* **2022**, *19*, 8240. [CrossRef] [PubMed]
27. Duke, G.D.; Kienzle, S.W.; Johnson, D.L.; Byrne, J.M. Improving Overland Flow Routing by Incorporating Ancillary Road Data into Digital Elevation Models. *J. Spat. Hydrol.* **2003**, *3*, 23–49.
28. Zuo, J.-J.; Cai, Y.-L. An automated watershed delineations approach for plain river network regions: A case study in Shanghai. *Adv. Water Sci.* **2011**, *22*, 337–343.
29. Si, Q.; Brito, H.C.; Alves, P.B.R.; Pavao-Zuckerman, M.A.; Rufino, I.A.A.; Hendricks, M.D. GIS-Based Spatial Approaches to Refining Urban Catchment Delineation That Integrate Stormwater Network Infrastructure. *Discov. Water* **2024**, *4*, 24. [CrossRef]
30. Jian, J.; He, S.; Liu, W.; Liu, S.; Guo, L. A Refined Method for the Simulation of Catchment Rainfall–Runoff Based on Satellite–Precipitation Downscaling. *J. Hydrol.* **2025**, *653*, 132795. [CrossRef]
31. Zhu, H.; Chen, Y. A Study of the Effect of DEM Spatial Resolution on Flood Simulation in Distributed Hydrological Modeling. *Remote Sens.* **2024**, *16*, 3105. [CrossRef]
32. Pareta, K.; Pareta, U. Evaluation of Stream Ordering Systems in the Context of Topography and Open-Source Data. *Earth Surf. Process. Landf.* **2024**, *49*, 3806–3821. [CrossRef]
33. Ma, J.; Zhou, F.; Yue, C.; Sun, Q.; Wang, X. The Coupled Application of the DB-IWHR Model and the MIKE 21 Model for the Assessment of Dam Failure Risk. *Water* **2024**, *16*, 2919. [CrossRef]
34. Zhang, Q.; Pang, G.; Long, Y.; Song, J.; Xing, L.; Yao, Y.; Xu, B.; Wang, L. Numerical Simulation and Validation of Heavy Rainfall Flood Inundation in Small Watersheds in Undocumented Mountainous Areas. *Hydrol. Res.* **2024**, *55*, 1271–1288. [CrossRef]
35. Xu, Y.; Ding, Y.-H.; Zhao, Z.-C. Prediction of Climate Change in Middle and Lower Reaches of the Yangtze River in the 21st Century. *J. Nat. Disasters* **2004**, *13*, 25–31.
36. Hossain, M.N.; Mumu, U.H. Flood Susceptibility Modelling of the Teesta River Basin through the AHP-MCDA Process Using GIS and Remote Sensing. *Nat. Hazards* **2024**, *120*, 12137–12161. [CrossRef]
37. Liu, X.; Wei, K. A Method for Calculating the Design Volume of the Initial Rainwater Storage Tank. *Water Resour. Manag.* **2025**, *39*, 161–177. [CrossRef]
38. Sene, A.P.; Caballero, J.A.; Ravagnani, M.A.S.S. A Novel and Efficient Mathematical Programming Approach for the Optimal Design of Rainwater Drainage Networks. *Water Resour. Manag.* **2025**, *39*, 883–905. [CrossRef]
39. Ennouini, W.; Fenocchi, A.; Petaccia, G.; Persi, E.; Sibilla, S. A Complete Methodology to Assess Hydraulic Risk in Small Ungauged Catchments Based on HEC-RAS 2D Rain-on-Grid Simulations. *Nat. Hazards* **2024**, *120*, 7381–7409. [CrossRef]
40. Shen, X.; Padua, M.; Zhang, B.; Kirkwood, N.; Song, Y.; Monacella, R. (Eds.) *Landscape Design, Evaluation and Management Created by Novel Technologies*; MDPI—Multidisciplinary Digital Publishing Institute: Basel, Switzerland, 2024.
41. Shen, X. Identifying the Role of Technology within the Discipline of 21st Century Landscape Architecture. *Des. J.* **2023**, *26*, 351–361. [CrossRef]